Exploiting Microscopic Spectrum Opportunities in Cognitive Radio Networks

Tao Shu and Marwan Krunz
Department of Electrical and Computer Engineering
University of Arizona

***Abstract*—In this paper, we are interested in cognitive radio networks (CRNs) whose operation does not rely on channel sensing. A spectrum server is responsible for collecting spectrum availability and location information from primary radio networks (PRNs), and broadcasting this information to cognitive radios. By subscribing to this broadcast, a CR knows about the spectrum opportunities without sensing channels. Spectrum opportunity under this paradigm presents a multi-level structure that generalizes the well-known channel-sensing-based binary structure. This multi-level structure reflects a *microscopic* spectrum opportunity for CRs, and can be exploited to increase the CRN throughput. Under this structure, we study efficient spectrum access in a multi-CR environment, with the objective of maximizing the network-wide utilization of spectrum opportunity. The difficulty of our problem comes from the fact that different CRs may decide the same channel to be available, but at different levels. Therefore, channel access needs to be carefully coordinated. Both centralized and distributed solutions are provided, supporting different modes of operation. Numerical results verify the accuracy of our algorithms and the significant gain achieved by the multi-level framework.**

I. Introduction

Cognitive radios (CRs) have been proposed as an enabling technology for opportunistic spectrum access (OSA). These radios are capable of identifying idle frequency bands (channels) and dynamically hoping between them to avoid interfering with the licensed users of the channel (a.k.a., primary radios (PRs)). To guarantee an interference-free reuse of the spectrum, channel sensing has long been considered as an indispensable component in the realization of CRs. For example, the IEEE 802.22 WRAN, the first standard for cognitive radio networks (CRNs), relies on distributed channel sensing to identify transmission opportunities.

In this paper, we are interested in a fundamentally different paradigm for utilizing unused spectrum. Specifically, we consider CRNs whose operation does not rely on channel sensing. We consider a spectrum-leasing scenario, where a CRN shares the spectrum with an infrastructure-based PRN, such as a cellular IS-95 or 802.16 WiMax system (see Figure 1). The PRN consists of multiple static base stations (BSs) that are interconnected via a broadband wired network, and member mobile stations (MSs, not shown in the figure) that communicate through wireless links with one of these BSs. We assume that each BS covers a certain area (i.e., a cell) and has the location information of itself and its member MSs. The BS periodically reports the spectrum utilization status of its cell, i.e., the instantaneous channel allocation among member MSs, as well as their location information, to a spectrum server via the wired network. The location of PR stations and the collected spectrum-status information are broadcasted by the server. By subscribing to this broadcast, a CR knows about the spectrum opportunities it can use without conducting channel sensing.

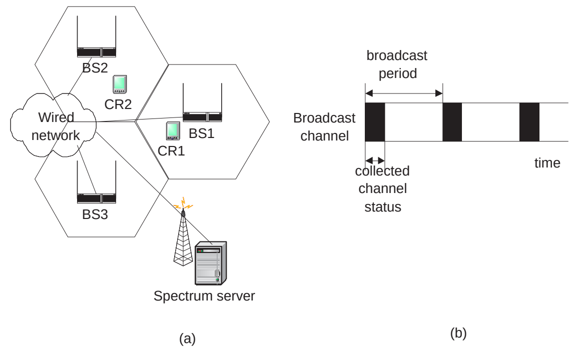

Fig. 1. Spectrum leasing: (a) System structure, (b) Timing of the broadcast of channel-status information from the spectrum server.

In contrast to the conventional channel-sensing-based paradigm, which assumes that the PRN is ambivalent to the existence of the CRN and no information exchange takes place between the two, the new paradigm assumes that the PRN collaborates with the CRN in identifying spectrum opportunities. This collaboration can be justified by *economic* considerations, where a PRN opens its spectrum to secondary reuse for a profit. The subscription component in the new paradigm is extremely suitable for implementing fee-based services, and thus provides a good incentive for the PRN to collaborate. This paradigm is also motivated by the following practical considerations: First, many existing PRNs are infrastructure based, and follow the architecture depicted in Figure 1. Location information of nodes are readily available in these systems [14]. Some location-oriented applications are actually utilizing such information. Second, as will be clear shortly, significant throughput gains can be achieved under this paradigm over conventional channel-sensing-based CRN systems. Third, low hardware complexity (and cost) is required at the CRs, because the sensing functionality can now be removed from it.

The subscription-based paradigm described in Figure 1 is in line with the CRN operational model recently advocated by the FCC [4], which calls for establishing a database that CR systems must first register with. This database provides a registered CR spectrum and geo-location information of PRs, and assists the CR in identifying spectrum opportunities. Note that the idea of a database-assisted method is still in its conceptual form. Quantitative knowledge of the benefit of this idea still needs to be realized, and its implementation details are yet to be developed.

Spectrum opportunity in the above framework presents a unique structure. Specifically, for each CR and each channel, we adopt a *power mask* to describe the maximum transmission power the CR can use without causing unacceptable interference to neighboring PRs. Due to the availability of the PR location information, this power mask is *multi-leveled*. For

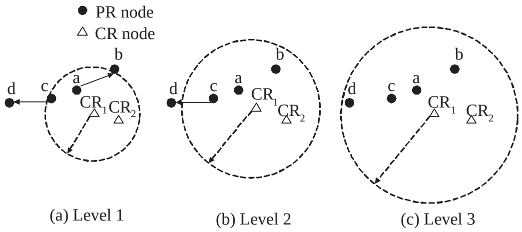

Fig. 2. Example of the multi-level spectrum opportunity (circles denote various interference ranges).

example, consider the scenario in Figure 2, where two PR links ($a \rightarrow b$ and $c \rightarrow d$) and one CR link (CR1 $\rightarrow$ CR2) operate in the same vicinity and share the same frequency channel. CR1 can transmit as long as its received power at the closest active PR receiver is smaller than the PR's interference tolerance, which is typically small and known. So depending on the status (ON/OFF) of the PR links, CR1's power mask takes one of three levels: $\frac{\text{PR's interference tolerance}}{h_{1b}}$ (Level 1), $\frac{\text{PR's interference tolerance}}{h_{1d}}$ (Level 2), and $P_{\max}$ (Level 3, the full power supported by the CR's battery), where h_{ij} is the channel gain between nodes i and j. Note that this multi-level structure is a generalization of the well-known *binary* structure, which uses channel sensing to identify spectrum opportunities and implements a binary power mask (0 if neighboring PR is active and $P_{\max}$ if none of them is active).

In this paper, we study the spectrum access problem in a CRN under the multi-level spectrum opportunity setup. Compared with the binary opportunity structure, we realize that this multi-level structure reflects *microscopic* spatial opportunity for CRs, and can be exploited to increase the CRN throughput. The difficulty of our problem comes from the fact that different CRs may consider the same channel to be available, but at different levels. Therefore, channel access needs to be carefully coordinated between these CRs to avoid collisions, and more importantly, ensure efficient utilization of the spectrum opportunity from a network-wide standpoint.

We formulate the coordinated channel access problem as a a joint power/rate control and channel assignment optimization problem. Different from previous works that investigated the problem mainly from a high-level mathematical viewpoint, our solutions are tailored to support two operational modes for CR systems, as specified by the FCC report [4]: (1) Centralized coordination (CC), and (2) distributed coordination (DC). In the CC mode, the spectrum server acts like a central controller. It not only collects spectrum and location information from the PRN, but also computes the transmission parameters, including transmission power, rate, and channel allocation, for each CR. As a result, no computation is required by the CR. For the DC mode, the spectrum server acts as a raw-information distributor; it only broadcasts PR locations and spectrum utilization information. Coordination among CRs is conducted in a distributed way, based on local computations of individual CRs. Because the CC mode provides better performance and DC mode provides better implementability for large-scale systems, we are interested in both.

The contributions of this paper are as follows. First, we show that the joint power/rate control and channel assignment problem can be formulated as an NP-hard mixed integer nonlinear programming (MINLP) problem. By exploiting the discrete set of rates supported by the CR on each channel, we transform this MINLP to a binary linear programming (BLP) problem that only contains binary variables and linear objective function and constraints. This transformation applies to any arbitrarily given rate-SINR relationship. We then develop two polynomial-time approximate algorithms for the BLP. The first one is the centralized *LPSF* algorithm. It is based on iteratively solving a series of linear programming problems and sequentially fixing the variables to either 1 or 0 in each iteration. The second is the distributed *EF-based* algorithm. This algorithm involves iterative and on-line adjustment of the power/rate of each CR over each channel based on some *economic factor* that accounts for the efficiency of investing power on a given channel. We show that this distributed algorithm is provably efficient, i.e., it can achieve a provable fraction of the optimal performance. Simulation results show that the actual performance gap is less than 10% in all simulated realizations. Our numerical results show that significant throughput gain (e.g., over 100% at best) can be achieved under the multi-level spectrum opportunity structure after accounting for the overhead of broadcast and subscription.

The rest of this paper is organized as follows. We review the related work in Section II. We describe the models and formulate the optimization problem in Section III. The BLP transformation, and the LPSF and EF algorithms are presented in Section IV. We describe the computation of power mask in Section V. Simulation results and discussion are provided in Section VI, and we conclude the work in Section VII.

II. Related Work

Much of the related work is based on the binary-type spectrum opportunity. Early works provide collision-free channel assignment for CR nodes given a set of available channels at each node. This problem can be described as an interference-graph vertex-coloring problem [15], [23]. To obtain a fast solution, various distributed approximations were proposed, which are based on observing local interference patterns [22], local bargaining [1], or on coordinations between CR nodes that aim at maximizing some system utility [2][19]. Because of the graph-theoretic nature of these algorithms, they take transmission power as input rather than output, and thus are not applicable to power/rate control problems.

The second body of work considers the sensing/channel access decision-making process from a single CR's viewpoint. This is also termed as *MAC-layer sensing*. Existing works include the partially observable Markov decision process (POMDP) model [21], the constrained Markov decision processes (CMDPs) model [20], and the optimal stopping-rule models [3] [7]. Assuming a semi-Markov process for the PR traffic, Kim and Shin [8] proposed a sensing-period adaptation algorithm that maximizes the discovery of spectrum opportunities and minimizes the delay in finding an available channel. Based on a similar PR traffic model, the authors in [6] studied a dynamic access scheme subject to a constraint on the CR-to-PR violation rate, but only for a system of one PRN and one CR link. The coordinated use of spectrum opportunities at neighboring CRs has not been considered in these works, and collisions between CR transmissions are resolved using standard CSMA/CA techniques. Such treatment leads to non-optimal performance from a network's viewpoint.

The third type of work simplifies the problem by restricting the treatment to CR nodes only. So the CR-to-PR and PR-to-CR interferences do not appear in their formulation. Within this category, Hou et al. [5] considered the joint optimization of spectrum, scheduling, and routing in a multi-hop software-defined-radio (SDR) network. Yi and Hou studied the joint optimization of power control, scheduling, and routing for a multi-hop SDR network in [10] (for a centralized algorithm) and [11] (for a distributed algorithm). Yuan et al. [18] introduced the concept of time-spectrum blocks to study spectrum allocation in CRNs. Based on a continuous-time Markov model, Xing et al. [16] proposed a random access protocol that achieves airtime fairness among CRs. The work in [17] considers spectrum access for CRs under an interference temperature constraint. However, because this constraint is defined only at a single location, compliance to it does not necessarily prevent interference on PR nodes.

III. System Model and Problem Formulation

We consider a distributed (ad hoc) CRN that coexists with M legacy (fixed spectrum) infrastructured PRNs over a finite area. PRN m, $m = 1, \ldots, M$, is licensed to operate over its own frequency channel of bandwidth B_m. In reality, a PRN may occupy more than one frequency channel. Such a network can be easily captured in our model by using multiple (virtual) PRNs that operate over different channels.

Let the number of CR links in the system be N. A CR link refers to a pair of CR sender and a CR receiver. For CR link i, we denote the sender and the receiver by $S(i)$ and $D(i)$, respectively. A CR link can transmit over multiple non-contiguous channels simultaneously. Let the transmission power on channel m be $P_i^{(m)}$. To avoid unacceptable CR-to-PR interference, this transmission power must be constrained below certain power mask $\hat{P}_i^{(m)}$. The value of $\hat{P}_i^{(m)}$ is related to the status of neighboring PRs and thus changes over time. For now, we assume that the value of $\hat{P}_i^{(m)}$s, $i = 1, \ldots, N$ and $m = 1, \ldots, M$, are given in each snapshot as input parameters of the joint power/rate control and channel assignment problem. We consider the calculation of $\hat{P}_i^{(m)}$ in Section V.

We stick to the *protocol model* for the collisions between CRs. We say that CR links i and j are interfering links on channel m if $\hat{P}_i^{(m)} h_{S(i)D(j)} > P_{I,CR}$ or $\hat{P}_j^{(m)} h_{S(j)D(i)} > P_{I,CR}$, where $h_{S(i)D(j)}$ and $h_{S(j)D(i)}$ are the cross-link channel gains of the two links, and $P_{I,CR}$ is a small fixed value, denoting the sensitivity of the CR receiver. Any received power below $P_{I,CR}$ can be deemed as ignorable in terms of interference. We assume that an exclusive channel occupancy policy is used to resolve collision between CRs: For any two interfering CR links on channel m, only one of them can access the channel at any given time.

Treating interference as noise, the rate of CR link i on channel m is given by

$$R_i^{(m)} = B_m f\left(\frac{P_i^{(m)} h_i^{(m)}}{q_{D(i)}^{(m)} + N_0}\right) \tag{1}$$

where f is any arbitrary rate-SINR function decided by the PHY-layer implementation, $h_i^{(m)}$ is the channel gain of link i on channel m, $q_{D(i)}^{(m)}$ is the received interference over channel m at $D(i)$, and N_0 is the AWGN. Because an exclusive channel occupancy policy is used, the interference $q_{D(i)}^{(m)}$ only comes from active co-channel PRs and can be measured by the CR receiver $D(i)$ on line.

For $i = 1, \ldots, N$ and $m = 1, \ldots, M$, define variables

$$x_i^{(m)} \stackrel{\text{def}}{=} \begin{cases} 1, & \text{if channel } m \text{ is used by CR link } i \text{, i.e., } R_i^{(m)} > 0 \\ 0, & \text{otherwise} \end{cases} \tag{2}$$

Our objective is to maximize the sum of rate of all CR links over all channels in current snapshot, i.e.,

$$\text{maximize} \sum_{i=1}^{N}\sum_{m=1}^{M} x_i^{(m)} R_i^{(m)} \tag{3}$$

where the maximization is to be carried out with respect to $x_i^{(m)}$'s and $R_i^{(m)}$'s.

A CR link i should satisfy the following constraints:

C1: CR-to-PR constraint: The transmission power of link i on channel m should not exceed the power mask $\hat{P}_i^{(m)}$. From (1), this constraint can be written in terms of $R_i^{(m)}$ as

$$\frac{1}{h_i^{(m)}}(q_{D(i)}^{(m)} + N_0) f^{-1}(r_i^{(m)}) \le \hat{P}_i^{(m)}, \quad m = 1, \ldots, M \tag{4}$$

where f^{-1} is the inverse function of f, and $r_i^{(m)} = \frac{R_i^{(m)}}{B_m}$ is the spectrum efficiency of link i on channel m.

C2: Power supply constraint: The sum of the transmission powers over all channels should not exceed the maximum power provided by the battery, i.e.,

$$\sum_{m=1}^{M} \frac{1}{h_i^{(m)}}(q_{D(i)}^{(m)} + N_0) f^{-1}(r_i^{(m)}) \le P_{\max,i}. \tag{5}$$

C3: CR-to-CR collision constraint: If channel m is being used by CR link i, then it cannot be used by another CR link that interferes with link i on channel m, and vice versa:

$$x_i^{(m)} + x_j^{(m)} \le 1, \quad \forall j \in I_i^{(m)} \tag{6}$$

where $I_i^{(m)} = \left\{j : j \ne i, \hat{P}_i^{(m)} h_{S(i)D(j)}^{(m)} > P_{I,CR}\right\} \cup \left\{j : j \ne i, \hat{P}_j^{(m)} h_{S(j)D(i)}^{(m)} > P_{I,CR}\right\}$ is the set of interfering CR links of link i on channel m.

C1 to C3 are the basic constraints that apply to all CRNs. Additional constraints may exist depending on the CR's PHY-layer implementation. For simplicity, we only include C1 to C3 to our formulation at this point. We will discuss other constraints in Section IV-D.

IV. Solutions

A. Transformation to BLP

An observation of the objective function (3) and the constraints C1-C3 shows that this formulation constitutes a *mixed integer nonlinear programming (MINLP)* problem. The solution to such a problem is NP-hard, in general. To make this formulation more amenable for further processing, we exploit the fact that actual communication systems only support a finite set of discrete transmission rates on each channel. Denote this set of rates by $\mathbf{U} = \{0, u_1, u_2, \ldots, u_K\}$ (in b/s/Hz), where $0 < u_1 < \ldots < u_K$. Define $\gamma_k \stackrel{\text{def}}{=} f^{-1}(u_k)$ for $k = 1, \ldots, K$; γ_k is the received symbol energy to interference plus noise density ratio (E_S/I_0) required to support the kth rate under the power-rate relationship defined by (1). Let $C_i^{(m)} \stackrel{\text{def}}{=} \frac{1}{h_i^{(m)}}\left(q_{D(i)}^{(m)} + N_0\right)$ for $i = 1, \ldots, N$ and $m = 1, \ldots, M$. $C_i^{(m)}$ is a known quantity for each CR link on each channel. We further define a new variable $y_{k,i}^{(m)}$ for all $k=1,\ldots,K$, $i=1,\ldots,N$, and $m=1,\ldots,M$:

$$y_{k,i}^{(m)} \stackrel{\text{def}}{=} \begin{cases} 1, & \text{if link } i \text{ is transmitting on channel } m \text{ using rate } u_k \\ 0, & \text{otherwise.} \end{cases} \tag{7}$$

In addition, we add the following constraint on $y_{k,i}^{(m)}$:

$$\sum_{k=1}^{K} y_{k,i}^{(m)} \leq 1. \tag{8}$$

which accounts for the fact that a link can use at most one rate on a given channel at a time. It is easy to show that the following relation holds:

$$x_i^{(m)} = \sum_{k=1}^{K} y_{k,i}^{(m)}. \tag{9}$$

Similarly, we can rewrite the spectrum efficiency $r_i^{(m)}$ in terms of $y_{k,i}^{(m)}$ and u_k:

$$r_i^{(m)} = \sum_{k=1}^{K} u_k y_{k,i}^{(m)}. \tag{10}$$

Substituting (9) and (10) into (3) through (6), we get the following equivalent formulation to the original MINLP problem:

$$\begin{array}{lll} & \text{maximize} & \sum_{i=1}^{N}\sum_{m=1}^{M}\sum_{k=1}^{K} B_m u_k y_{k,i}^{(m)} \\ & \text{such that} & \\ \tilde{C}1: & & C_i^{(m)} \sum_{k=1}^{K} \gamma_k y_{k,i}^{(m)} \leq \hat{P}_i^{(m)} \\ \tilde{C}2: & & \sum_{m=1}^{m} C_i^{(m)} \sum_{k=1}^{K} \gamma_k y_{k,i}^{(m)} \leq P_{\max,i} \\ \tilde{C}3: & & \sum_{k=1}^{K} y_{k,i}^{(m)} + \sum_{k=1}^{K} y_{k,j}^{(m)} \leq 1, \quad \forall j \in I_i^{(m)} \end{array} \tag{11}$$

where the maximization is w.r.t. the $y_{k,i}^{(m)}$'s.

An examination of (11) shows that the former MINLP problem has been transformed into a binary linear program (BLP) that contains only binary variables and linear objective function and constraints. A nice property of (11) is that the rate levels u_k, $k=1,\ldots,K$, and the corresponding γ_k's are fed into the BLP formulation as tuples (u_k,γ_k). In other words, the BLP formulation does not rely on the specific functional relationship between u_k and γ_k, and thus can accommodate any arbitrary rate-power relation (e.g., a staircase-like function that characterizes practical multi-rate systems).

B. LPSF Centralized Algorithm

A BLP is a combinatorial problem. Its solution, in general, is NP-hard. A typical algorithm to approximately solve this problem is the so-called *branch-and-bound* algorithm, whose worst-case time complexity is exponential.

Instead of employing a branch-and-bound algorithm, we develop polynomial-time approximate algorithms by exploiting the special structure of the problem. An observation of (11) indicates that if we relax $y_{k,i}^{(m)}$'s from their binary values and allow them to take real values between 0 and 1, then the formulation becomes a linear program (LP) that is solvable in polynomial time. In addition, the constraint $\tilde{C}3$ dictates that if for some m, k, and i, $y_{k,i}^{(m)}=1$, then $y_{h,i}^{(m)}=0$ for all $h\neq k$ and $y_{l,j}^{(m)}=0$ for all $j\in I_i^{(m)}$ and $1\leq l\leq K$. In other words, a strong dependence exists between the $y_{k,i}^{(m)}$'s that belong to the same interfering CR link set. The main idea behind our fast approximate solution is to fix the values of $y_{k,i}^{(m)}$'s sequentially through solving a series of relaxed LP problems, with at least one $y_{k,i}^{(m)}$ finalized to a binary value at each iteration.

Our approximation algorithm, called LP with sequential fixing (LPSF), is described in Table I. In the first iteration, we append the constraint $0\leq y_{k,i}^{(m)}\leq 1$ to (11) and relax all $y_{k,i}^{(m)}$'s to real values between 0 and 1. We refer to the resulting formulation as LP$^{(1)}$, which must have a feasible solution according to Lemma 1. The solution to LP$^{(1)}$ is an upper bound on the optimal solution to (11), because the feasibility region of the BLP is a subset of that of LP$^{(1)}$. However, the solution of LP$^{(1)}$ is, in general, not a feasible solution to the original BLP problem, because the $y_{k,i}^{(m)}$'s can now take values between 0 and 1. Among all $y_{k,i}^{(m)}$'s, we pick the one that has the largest value, and we denote this $y_{k,i}^{(m)}$ by $Y_{k,i}^{(m)}$ for ease of identification. We set $Y_{k,i}^{(m)}=1$. Accordingly, all $y_{h,i}^{(m)}$'s for $h\neq k$ and all $y_{l,j}^{(m)}$'s for $j\in I_i^{(m)}$ and $1\leq l\leq K$ must now be set to 0. Substituting these $y_{k,i}^{(m)}$'s with their fixed values into the LP$^{(1)}$, we get a new LP, called LP$^{(2)}$, whose variables do not include those that have been fixed after the execution of LP$^{(1)}$ (such variables have been replaced by their binary values). A feasibility check is then conducted on LP$^{(2)}$. If the feasible region of LP$^{(2)}$ is empty, that means the first fixing in this iteration, i.e., $Y_{k,i}^{(m)}=1$, is not correct. So we reset $Y_{k,i}^{(m)}$ to 0. This change means all those variables that belong to the same interfering CR link set as $Y_{k,i}^{(m)}$ and whose values have been fixed to 0 in this iteration must now become variables. The revised fix, i.e. $Y_{k,i}^{(m)}=0$, is then substituted into LP$^{(1)}$, giving rise to LP$^{(3)}$. LP$^{(3)}$ must be feasible (see Lemma 2). In a nutshell, at this point we either have a feasible LP$^{(2)}$ or have a feasible LP$^{(3)}$. In either case, the new feasible formulation is renamed as LP$^{(1)}$ and a new iteration starts following the same process above. The process is repeated until all $y_{k,i}^{(m)}$'s are set to either 0 or 1. The final rate allocation of each link on each channel is calculated according to (10).

STEP 0: Get LP$^{(1)}$ by appending $0\leq y_{k,i}^{(m)}\leq 1$ to (11) and relaxing all variables to real values.
STEP 1: Solve LP$^{(1)}$.
STEP 2: Pick $Y_{k,i}^{(m)} \Leftarrow \max\left\{y_{l,j}^{n}, l\in(1,\ldots,K), j\in(1,\ldots,N), n\in(1,\ldots,M)\right\}$.
STEP 3: Get LP$^{(2)}$ by substituting $Y_{k,i}^{(m)}=1$, $y_{h,i}^{(m)}=0$ for $h\neq k$ and $y_{l,j}^{(m)}=0$ for $\forall j\in I_i$ and $1\leq l\leq K$ into LP$^{(1)}$.
STEP 4: If LP$^{(2)}$ is feasible
  LP$^{(1)}$ $\Leftarrow$ LP$^{(2)}$
 else
  Get LP$^{(3)}$ by substituting $Y_{k,i}^{(m)}=0$ into LP$^{(1)}$.
  LP$^{(1)}$ $\Leftarrow$ LP$^{(3)}$
 End-if
STEP 5: If all variables are fixed, then **Terminate**; otherwise go to **STEP 1**.

TABLE I
LPSF ALGORITHM.

Theorem 1: The LPSF algorithm can correctly determine the binary values of all $y_{k,i}^{(m)}$'s in no more than NMK iterations.

The proof of Theorem 1 is based on the following lemmas.

Lemma 1: In the first iteration, LP$^{(1)}$ has an optimal solution.

Proof: It is easy to show that at least $y_{ki}^{(m)}=0$ for all $k=1,\ldots,K$, $i=1,\ldots,N$, and $m=1,\ldots,M$, is a feasible solution to the original BLP. Thus it is also a feasible solution to LP$^{(1)}$. Note that all variables are bounded between [0, 1], therefore Lemma 1 holds. ∎

Lemma 2: In the first iteration, LP$^{(3)}$ has an optimal solution.

Proof: According to Lemma 1, LP$^{(1)}$ in the first iteration must have optimal solution, therefore $Y_{ki}^{(m)} \geq 0$ must holds before the fix. When $Y_{ki}^{(m)}$ is fixed to 0 to get LP$^{(3)}$, its value is changed from no less than 0 to 0, leading to a non-increase in the required transmission power. So no R.H.S. of C1' through C3' could be violated by this non-increasing action on the L.H.S. of C1' through C3'. Therefore LP$^{(3)}$ must have at least one feasible solution. Noting that all variables are bounded between [0, 1], Lemma 2 holds. ∎

Lemma 3: LP$^{(1)}$ and LP$^{(3)}$ have optimal solutions in all iterations.

Proof: The situation in the first iteration is proved by Lemma 1 and Lemma 2. In the second iteration, LP$^{(1)}$ comes from either a feasible LP$^{(2)}$ or a feasible LP$^{(3)}$ of the first iteration. So LP$^{(1)}$ must be feasible in the second iteration. Given LP$^{(1)}$ is feasible in the second iteration, the rational used in proving Lemma 2 also applies here to prove the feasibility of LP$^{(3)}$ in the second iteration. This induction repeats itself in all iterations. Noting that all variables are bounded between [0, 1], Lemma 3 holds. ∎

The proof of Theorem 1 is straightforward: Iteratively applying Lemmas 1 to 3, it is guaranteed that in each iteration at least one $y_{ki}^{(m)}$ is fixed to either 0 or 1 and a new feasible LP$^{(1)}$ is generated for the next iteration. For the last iteration, if fixing $y_{ki}^{(m)}$ to 1 does not lead to a feasible BLP solution, then changing its value to 0 must lead to a feasible BLP solution (due to the same reason as in the proof of Lemma 2). ∎

Based on Theorem 1, it is easy to show that the time complexity of the LPSF algorithm is bounded by the complexity of the LP solver times NMK. Because a LP solver has polynomial complexity, the complexity of the LPSF is also polynomial. In addition, the performance gap between the approximate solution and the actual optimum can be explicitly evaluated by comparing against the upper bound of the optimal solution, which is the the solution to LP$^{(1)}$ in the first iteration. Lemma 1 has guaranteed the existence of this upper bound. We will shortly show by simulation that this gap is very small (below 10%), and in most cases it is zero.

C. Distributed Algorithm

In this section, we develop a provably efficient distributed algorithm for the BLP problem (11), which can achieve a provable fraction of the optimal performance. The intuition behind such an algorithm stems from understanding the conflicts between CRs in utilizing spectrum opportunities. There are two main reasons for such conflicts. First, neighboring CRs may observe a similar level of spectrum availability over a given channel, and thus may attempt to transmit simultaneously over the same channel, causing collisions. Second, transmissions by the same CR over different channels may also conflict with each other, in the sense that the maximum transmission power provided by the battery may not be sufficient to support parallel transmissions over all these channels. In a nutshell, conflicts between transmissions occur due to their competition for both frequency and power resources. A good design philosophy is to give priority to a transmission that can contribute higher rate at a lower power. Following this philosophy, the proposed distributed algorithm defines an *economic factor* (EF) for each channel at each CR link. Let the current rate level of link i on channel m be $r_i^{(m)} = u_k$, where $k = 0, \ldots, K-1$. Then, the EF of this channel is defined as

$$\eta_i^{(m)} \stackrel{\text{def}}{=} \frac{\Delta P_i^{(m)}}{B_m \Delta r_i^{(m)}} = \frac{C_i^{(m)}(\gamma_{k+1} - \gamma_k)}{B_m(u_{k+1} - u_k)}. \quad (12)$$

We define $\eta_i^{(m)} \stackrel{\text{def}}{=} +\infty$ for $r_i^{(m)} = u_K$.

/* CR link i */
Initialization: $r_i^{(m)} \Leftarrow 0$, for $m = 1, \ldots, M$ and $\mathcal{C} \Leftarrow \{1, \ldots, M\}$

while ($\mathcal{C} \neq \emptyset$)
  /* Internal candidate selection */
  $violation\_flag \Leftarrow 1$
  while ($violation\_flag == 1$)
    $m^* \Leftarrow \arg\min \left\{ \eta_i^{(m)} | m \in \mathcal{C} \right\}$
    calculate $\Delta P_i^{(m^*)}$
    if (($\Delta P_i^{(m^*)} + P_i^{(m^*)} \leq \hat{P}_i^{(m^*)}$)
    or ($\Delta P_i^{(m^*)} + \sum_{m=1}^{M} P_i^{(m)} \leq P_{max,i}$))
      $violation\_flag \Leftarrow 0$
    else
      $\mathcal{C} \Leftarrow \mathcal{C} - \{m^*\}$
    end-if
  end-while

  /* Inter-link selection */
  exchange with neighbors the message (link id $i \|$channel id $m^* \parallel \eta_i^{(m^*)}$)
  if ($\eta_i^{m^*}$ is the minimum among neighbors)
    increase $r_i^{(m^*)}$ from u_k to u_{k+1}
    if ($r_i^{(m^*)} == u_K$)
      $\mathcal{C} \Leftarrow \mathcal{C} - \{m^*\}$
    end-if
    send rate-adjustment message
  end-if

  /* Collision elimination routine */
  if (a rate-adjustment message is received from link j)
    calculate $h_{S(j)D(i)}$ based on received signal strength
    if ($h_{S(j)D(i)} \hat{P}_j^{(m^*)} > P_{I,CR}$)
      if ($r_i^{(m^*)} \leq r_j^{(m^*)}$)
        $r_i^{(m^*)} \Leftarrow 0$ and $\mathcal{C} \Leftarrow \mathcal{C} - \{m\}$
      else
        $S(i)$ sends a rate-adjustment message
      end-if
    end-if
  end-if
end-while
Output: $r_i^{(m)}$, for $m = 1, \ldots, M$

TABLE II
PSEUDO-CODE FOR THE EF-BASED DISTRIBUTED ALGORITHM.

The basic idea of our EF-based distributed algorithm is to iteratively ramp up the rate level over each channel of every neighboring link until the power mask and maximum-power constraints are violated. In each iteration, the link-channel pair that has the smallest EF value among its interfering-link set is raised to the next higher rate. This is achieved by sequentially executing the following three procedures in each iteration (note that this algorithm is executed in parallel at various CR transmitters). The first procedure is an *internal candidate selection* process, where a link, say i, selects a channel m^* that has the smallest EF among all channels in a *candidate channel set* $\mathcal{C}$. The set $\mathcal{C}$ is initialized to contain all M channels. The selected channel m^* is tested for the feasibility of a rate increase: This is done by calculating the increment of transmission power $\Delta P_i^{(m^*)} = C_i^{(m^*)}(\gamma_{k+1} - \gamma_k)$. If this transmission power increment violates the power mask or the battery power constraint, then a rate increase on channel m^* is infeasible for the CR. So m^* will be deleted from $\mathcal{C}$ and the above selection process is repeated. Eventually, either a feasible m^* will be selected or $\mathcal{C}$ becomes empty. When $\mathcal{C}$ becomes empty, the iterative process at the CR transmitter terminates. In case a feasible m^* is found, the algorithm enters the *inter-link selection* phase.

In the inter-link selection phase, neighboring CR transmitters exchange the results of their internal selection to elect the link-channel pair that has the smallest EF among the neighborhood. The internal selection result of a link i is broadcasted in the following format (link id $i \|$channel id $m^* \parallel \eta_i^{(m^*)}$), where $\|$ means concatenation. The link-channel pair that has the smallest EF in its neighborhood raises the corresponding rate by one level, i.e., from u_k to u_{k+1}. At the same time, the sender of this link, say $S(j)$, will broadcast in full power $P_{\max,j}$ the following *rate-adjustment* message to its neighbors: (link id j $\|$ channel id $m^* \parallel r_j^{(m^*)} \parallel \hat{P}_j^{(m^*)} \parallel P_{\max,j}$).

Whenever a CR link i receives a rate-adjustment message from link j, it performs a *collision elimination* routine. In particular, the receiver of the ith link, $D(i)$, will calculate the path loss from $S(j)$ (the sender of the message) to $D(i)$ based on the received signal strength of the message. Based on the power mask information in the message, $D(i)$ can then decide whether $S(j)$'s transmission will interfere with the reception at $D(i)$ on channel m. If so, $D(i)$ will compare $r_i^{(m^*)}$ with $r_j^{(m^*)}$. If $r_i^{(m^*)} \leq r_j^{(m^*)}$, then $D(i)$ notifies $S(i)$ to set $r_i^{(m^*)}$ to zero and delete m^* from $\mathcal{C}$. If $r_i^{(m^*)} > r_j^{(m^*)}$, then $D(i)$ notifies $S(i)$ to send a rate-adjustment message to trigger link j to eliminate channel m^* from its usage.

A pseudo-code description of the algorithm is given in Table II. Because at least one $r_i^{(m)}$ will be increased by one level in each iteration in each interfering-link set, the rate adjustment will terminate in at most MK iterations. In addition, Theorem 2 specifies the efficiency of this algorithm.

Theorem 2: The EF-based distributed algorithm can achieve at least $1/(\kappa^*+1)$ of the optimal performance, where $\kappa^* = \max_{i,m} |I_i^{(m)}|$ is the maximum interference degree of all CR links over all channels, $|\cdot|$ denotes the cardinality of the set.

Proof: The rate adjustment in the EF algorithm is analogous to the well-known single-user optimal Levin-Campello greedy algorithm [13] for bit loading in an OFDM system. In allocating each bit, this greedy algorithm calculates the cost to add one more bit in each subchannel and chooses the subchannel that requires the least cost, where the cost is the incremental power necessary. It has been shown in [9] that for multiuser multi-carrier systems, if we assume no interference exists between users, then the same greedy algorithm also achieves optimal performance. Denote the optimal sum of rate of this idealized non-interfering multiuser system by $R_{tot,\max}^{(0)}$, this sum is calculated as:

$$R_{tot,\max}^{(0)} = \sum_{i=1}^{N} \sum_{m=1}^{M} R_i^{(m)} \tag{13}$$

where $R_i^{(m)}$ are the output of the greedy algorithm when interference between users are ignored. When interference is accounted for, the third "if" statement in the collision-elimination routine of the EF-based algorithm (see Table II) guarantees that for every interfering link set, only the link that achieves the largest rate is remained (i.e., can access this channel), while all other interfering links are eliminated from using this channel (their rates on this channel are all set to 0). Denote by $Z^{(m)}$ the set of links that can access channel m when the EF algorithm is used. So for $\forall z \in Z^{(m)}$, it must be true that $R_z^{(m)} \geq R_j^{(m)}$ for $\forall j \in I_z^{(m)}$. When interference is accounted for, denote the sum of rate of the EF algorithm by $R_{tot,EF}^{(1)}$. Then $R_{tot,EF}^{(1)} = \sum_{m=1}^{M} \sum_{z\in Z^{(m)}} R_z^{(m)}$. We further have the following relationship:

$$\begin{aligned} R_{tot,\max}^{(0)} &= \sum_{m=1}^{M} \sum_{i=1}^{N} R_i^{(m)} \\ &\leq \sum_{m=1}^{M} \sum_{z\in Z^{(m)}} (|I_z^{(m)}|+1) R_z^{(m)} \\ &\leq \sum_{m=1}^{M} \sum_{z\in Z^{(m)}} (\kappa^*+1) R_z^{(m)} \\ &= (\kappa^*+1) R_{tot,EF}^{(1)} \end{aligned} \tag{14}$$

When interference exists between users, we denote the optimal sum of rate by $R_{tot,\max}^{(1)}$. Obviously,

$$R_{tot,\max}^{(1)} \leq R_{tot,\max}^{(0)} \leq (\kappa^*+1) R_{tot,EF}^{(1)}. \tag{15}$$

So it follows that $R_{tot,EF}^{(1)} \geq \frac{1}{\kappa^*+1} R_{tot,\max}^{(1)}$. Then Theorem 2 follows. ■

Theorem 2 shows that the EF-based algorithm is optimal when $\kappa^* = 0$, e.g., when any two CR links are separated far away such that they do not interfere with each other. When interference exists, the algorithm's performance lower bound decreases linearly with κ^*. The actual performance gap will be evaluated later on by simulations.

D. Additional Constraints

Depending on the CR's hardware capabilities or on some regulatory factors, additional constraints on the CRN may be imposed. These include:

C4: Number of Parallel Transmissions: The maximum number of channels a CR transmitter can use at one time may be bounded by M_t. In the BLP framework, this constraint is presented as

$$\tilde{C}4: \qquad \sum_{m=1}^{M} \sum_{k=1}^{K} y_{k,i}^{(m)} \leq M_t, \quad \text{for } i=1,\ldots,N. \tag{16}$$

C5: Transmission Bandwidth: The total bandwidth a CR can transmit over at one time is bounded by B_t. Formally,

$$\tilde{C}5: \qquad \sum_{m=1}^{M} \sum_{k=1}^{K} B_m y_{k,i}^{(m)} \leq B_t, \quad \text{for } i=1,\ldots,N. \tag{17}$$

C6: Forbidden Channels: A CR link i may be prohibited from using a certain set of channels, say $\mathbf{BF}_i \subseteq \{1,\ldots,M\}$. This constraint can be modeled as

$$\tilde{C}6: \qquad y_{k,i}^{(m)} = 0, \quad \text{for } k=1,\ldots,K, \text{and } m \in \mathbf{BF}_i. \tag{18}$$

An examination of (16) through (18) shows that the additional constraints are linear in the $y_{k,i}^{(m)}$'s. Thus, they do not fundamentally change the BLP formulation and its solutions discussed in previous sections. The extensions of the LPSF and the EF-based algorithms are trivial, and thus are ignored due to space limitation.

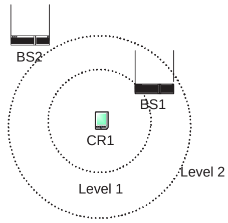

Fig. 3. Calculating the multi-level power mask.

V. Implementation Issues

In this section, we use the example in Figure 3 to illustrate the main idea of calculating the power mask under multi-level spectrum opportunity setup. We assume that the PRN operates using frequency division duplex (FDD). At any given time, the BS tunes to some of the M uplink channels to receive signals from the PR mobile stations (MSs) (not shown in the figure). We use the spectrum sharing of the uplink as the example. To be consistent with the model in Section III, a BS operating on multiple channels can be modeled as multiple virtual BSs that operate on individual non-overlapping channels.

The basic idea of computing the power mask is to adapt its interference range to the activity of neighboring PR BSs. The interference range is defined as the signal propagation distance d_I, such that $\hat{P}_i^{(m)} h^{(m)}(d_I) \leq P_I$, where $h^{(m)}(d_I)$ is the channel gain for distance d_I on channel m, and the interference tolerance P_I is a small value, below which the interference can be deemed as no harm to the PR. We also assume that each CR has the knowledge of its location, and thus can calculate its distance to neighboring PR BSs. The interference-range adaption is illustrated in Figure 3: If the channel gain is fully decided by the propagation distance, then when BS1 is receiving on channel m, CR1's power mask should be such that its interference range is right smaller than the distance between CR1 and BS1 (denoted as the smallest dotted circle (Level 1) in the figure). When BS1 is not receiving but BS2 is receiving, then the power mask can be increased such that its interference range reaches the larger dotted circle (Level 2), and so on. Although this basic idea seems straightforward, the calculation needs to take into account the following two random factors.

A. Randomness of PR Activity

This randomness impacts the choose of right level for the power mask. For example, in Figure 3, even if BS1's status on channel m is reported as not receiving at current reporting time, there is a chance that it subsequently flips to receiving before the next reporting time. This status change cannot be reflected to CRs until the next report. So if a CR is transmitting based on the power mask of Level 2, which is calculated directly according to current status report, then unacceptable interference will be caused to BS1, leading to a violation to the PRN. To account for this random violation, we impose a soft guarantee, $\alpha^{(m)}$ for channel m, such that the ratio of the time the CR violates PRN on channel m is smaller than $\alpha^{(m)}$. This constraint requires us to take into account the accumulated possibility of status-flipping (from not-receiving to receiving) of all idle BSs that are closer to the target CR than its closest active BS neighbor. As a result, it might not always be appropriate to use a power mask that corresponds to the closest active BS neighbor. For example, in Figure 3, even if BS2 is the closet active neighbor of CR1 in the current report, the CR should not use the power mask of Level 2, if the possibility of BS1 flipping to receiving is greater than $\alpha^{(m)}$. The detailed mathematical treatment is presented in our technical report [12], and is omitted here due to page limitation.

B. Randomness of the Channel Gain

This randomness impacts the value of each power mask level. Given $\hat{P}_i^{(m)}$, the random fluctuation of the channel makes the received signal strength after distance d_I a random variable: $\hat{p}_i^{(m)} = \hat{P}_i^{(m)} \bar{h}(d_I) \chi^{(m)}$, where $\chi^{(m)}$ is a unit-mean r.v. denoting the random fluctuation of the channel, $\bar{h}(d_I) = A_0 d_I^{-\mu}$ is the distance-related component of path loss, A_0 is the close-in constant, and μ is the path loss exponent. To counter this random effect, we impose a second soft guarantee, $\beta^{(m)}$ for channel m, which requires $\Pr\{\hat{P}^{(m)} \bar{h}(d_I) \chi^{(m)} \geq P_I\} < \beta^{(m)}$. Since d_I is fixed (this corresponds to the interference range of the level selected in last section), $\hat{P}_i^{(m)}$ is calculated as $\hat{P}_i^{(m)} = \frac{P_I}{\bar{h}(d_I) Q^{(m)}(\beta^{(m)})}$, where $Q^{(m)}(\beta^{(m)})$ is the $(1-\beta^{(m)})$-quantile of the fluctuation $\chi^{(m)}$, i.e., $\Pr\{\chi^{(m)} \leq Q^{(m)}(\beta^{(m)})\} = 1-\beta^{(m)}$.

Obviously, the frequency by which each BS reports to the spectrum server has an impact on the calculated power mask. The lower the frequency, the larger the uncertainty for the BS' status between two consecutive reports, and therefore the more conservative the power mask will be in order to guarantee the given PRN violation constraint. On the other hand, the bandwidth of the channel-status information broadcast channel also influences the throughput of the CRN: Because CRs update their power masks according to the periodic broadcast, the higher the broadcast bandwidth, the quicker each CR can acquire the channel-status information, thus more time left between two consecutive updates for a CR to deliver data. The interesting question is how much gain the multi-level scheme can attain when the overhead of the broadcast has been accounted for. We will answer this question based on simulations shortly.

VI. Performance Evaluation

A. Accuracy of the Approximate Algorithms

We consider a 1000×1000 meter^2 region, where 5 PRNs (5 channels) coexist with 5 CR links. The numbers of PRs over each channel are 25, 10, 15, 20, and 25, respectively. Each channel has 1 MHz of bandwidth. We assume the following rate-SINR relationship: $R_i^{(m)} = B_m \log_2(1 + SINR/8)$, and $r_i^{(m)} \in \{0, 1/2, 1, 3/2, 2\}$ bits/second/Hz for all i and m. The locations of the PR and CR transmitters and receivers are randomly assigned within the simulation region. A simple path loss model with exponent of 4 is assumed for the channel gain between any two points (i.e., $h_{ij} = d_{ij}^{-4}$). We assume the PRs on all channels follow the same 2-state Markov activity model, i.e., durations of ON/OFF states are exponentially distributed, with the average ON and OFF periods set to 1 s and 10 s, respectively. The transmission power of a PR is 500 mW. The $P_{\max}$ for a CR is 1 W. We assume the interference tolerance $P_I = 2P_{I,CR} = 0.12346$ μW. The PR's status report period is 100 ms and the CR-to-PR violation bound is $\alpha^{(m)} = 2\%$ for all m. A CR is capable of using all 5 channels at one time. We compare the sum-rate of all CR links achieved in each report period under 3 different algorithms: an exhaustive-search algorithm that finds the optimal solution, our polynomial-time LPSF algorithm, and the EF algorithm.

The CRN sum-rate is plotted in Figure 4 for 50 consecutive status report periods. We randomly choose to present this trace

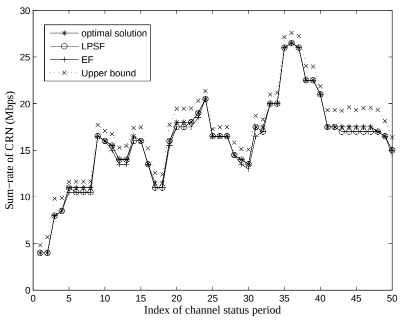

Fig. 4. Trace of the CRN's Sum-rate.

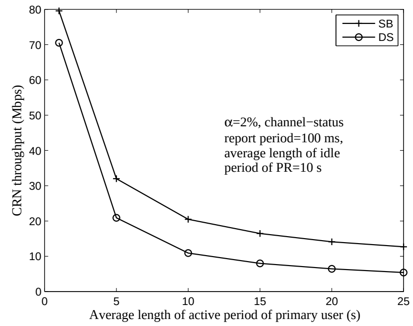

Fig. 5. CRN throughput vs. PR activity.

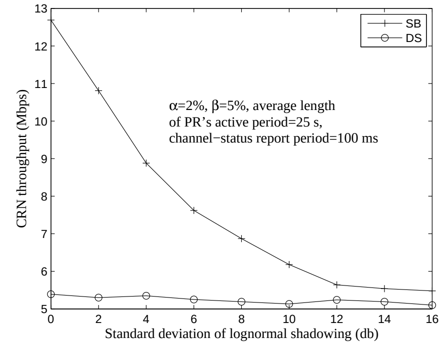

Fig. 6. CRN throughput vs. channel shadowing.

among the many we have simulated. The upper bound generated in the first iteration of the LPSF algorithm is also shown. It is clear that the LPSF and the EF algorithms give near-optimal solutions. In all cases, these solutions are within 5% from the optimal solution. In most of the cases their solution is the actual optimal solution. In addition, the upper bound provided by the LPSF algorithm is reasonably tight. In all simulations, the gap between this bound and the optimal solution does not exceed 10%. So this bound provides a useful reference to evaluate the accuracy of the approximate solutions in large networks when the optimal solution is computationally difficult to obtain.

B. Comparison between Binary and Multi-level Opportunities

Since getting the optimal solution is not our target in this section, we simulate a larger-scale system and apply EF algorithm for channel access. We consider 10 channels and 10 CR links over the same square area. The numbers of PRs on each channel are 25, 10, 15, 20, 25, 10, 5, 15, 20, and 25, respectively. In addition, the set of rates supported by a CR is now given by $\{0, 1/2, 1, 3/2, 2, 5/2, 3, 7/2, 4\}$ b/s/Hz. So the number of binary variables in the BLP is increased to 800. Unless indicated, the other parameters stay the same as before. In the following results, the conventional sensing-based CRN paradigm that yields a binary spectrum opportunity for CRs is referred to as DS (standing for distributed sensing) scheme. The new paradigm that leads to the multi-level spectrum opportunity is referred to as SB (subscription-based) scheme. The results presented are based on the average of 20 randomly generated topologies, with a simulation time of 1000 sensing/status-report periods for each topology.

We assume the channel-sensing period of DS scheme is 100 ms. We denote the status-report period of SB scheme by T. The performance matric of interest is the CRN throughput, defined as the average number of data bits that can be transmitted by all CR links in one period divided by the duration of the period. Because under the SB scheme, a fraction of the period, denoted by T_B, is used to receive broadcast information at each CR, the actual data transmission time in each period is $T - T_B$. The overhead is given by $T_B = \frac{V_B}{B_B}$, where V_B is the number of bits of the collected channel-status information in one report period, and B_B is the bandwidth of the broadcast channel. For our simulation, V_B is loosely upper bounded as follows: We assume that the channel-status information for one PR has the format (PR id ‖ channel id ‖ channel status). The total number of PRs is less than 200, so an id of 8 bits is enough to identify each of them. The total number of channels is 10, so 4 bits are enough to identify the channel a PR is working on, and 1 bit is used to identify the status of the PR (ON/OFF). So $V_B < 200 \times (8+4+1) = 2.6K$ bits. We use this value in our following calculation of the overhead. To give a conservative estimation of the gain attained by SB scheme, we assume that the channel sensing in DS scheme takes 0 time. Thus the throughput of the DS scheme plotted below represents the upper bound of any channel access schemes that are based on binary spectrum opportunity. We ignore the EF algorithm's computation time in both schemes.

In Figure 5, we study the CRN throughput as function of the PRs' activities. Here we fix $B_B = 260$ Kb/s, corresponding to $T_B = 10$ ms. It can be observed that at low PR activity, the throughput of SB exceeds DS slightly (a 15% gain); but at high PR activity, SB exceeds DS significantly (a 150% gain). So it is clear that although the broadcast channel consumes about 2.6% of the total system bandwidth, it leads to at least 15% throughput gain in worst case and 150% gain in best case scenarios. The difference of gains is because when PR activity is low, all neighboring PRs are often in the OFF state. The outcome of SB becomes similar to DS in the sense that most of the time a CR can use the highest power level $P_{\max}$ for transmission. With increased PR activity, the middle- and low-level power masks happen more and more frequently under the SB scheme, while DS observes more and more "0" (no transmission) opportunities, thus the gap between the two schemes keeps growing.

We study the impact of channel fluctuations in Figure 6, where a channel is subject to log-normal shadowing. The channel gain is now simulated by $g_{ij} = d_{ij}^{-4} 10^{\frac{\chi}{10}}$, where χ is a zero-mean Gaussian random variable denoting the channel fluctuation measured in decibel (db). The standard deviation of χ represents the severity of the shadowing. For each channel, we require the soft guarantee $\beta = 5\%$. We first note that the average throughput of DS barely changes with the fluctuation because it has a fixed power-mask set $(0, P_{\max})$. It is also observed that with the increase of channel fluctuation, the throughput under SB will decrease, and eventually it approaches to that of TOS. But when the standard deviation is 6 db, which is the value for a typical shadowing environment, SB still achieves about 50% throughput gain over DS.

In Figure 7, we fix $B_B = 260$ Kb/s (or $T_B = 10$ ms) and change the status-broadcast period as the variable. It can be observed that in general, a shorter broadcast period leads to a higher throughput because of the increased certainty of the PR's activity between two consecutive reporting moments. However, when the broadcast period is very small, e.g., $T = 40$ ms, the throughput of SB is low. This is because the broadcast of status information occupies a significant portion of each broadcast period, thus less time is left for data transmission.

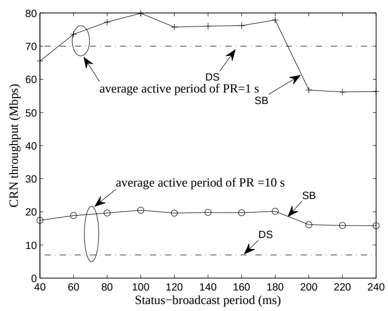

Fig. 7. CRN throughput vs. period of the status broadcast.

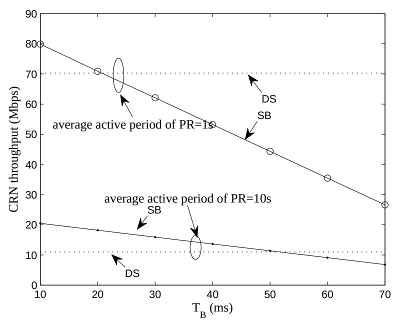

Fig. 8. CRN throughput vs. bandwidth of the broadcast channel.

In Figure 8, we fix the status-broadcast period $T = 100$ ms, and plot the throughput of SB under various T_B (corresponding to various broadcast channel bandwidth). It can be observed that the throughput of SB degrades linearly with the increase of T_B (or equivalently, the decrease of the broadcast bandwidth), because less and less fraction of time in each period is left for transmitting data. For low PR activity, the throughput of SB crosses that of DS after T_B is greater than 20 ms or B_B is smaller than 130 Kb/s, which is about 1.3% of the total system bandwidth. For high PR activity, the crossing point is $T_B = 50$ ms. This corresponds to $B_B \approx 50$ Kb/s (0.5% of the total bandwidth). The extremely small bandwidth at the crossing in both situations indicate that the overhead of SB is basically ignorable compared with the significant throughput gains it leads to.

VII. Conclusions

In this paper, we developed both centralized and distributed algorithms for the problem of coordinated channel access in a spectrum-server-assisted CRN. The problem is formulated under a multi-level spectrum opportunity framework that reflects the microscopic spatial opportunity available for CRs. We also applied our algorithms to study the throughput gains achieved by this multi-level framework over the conventional binary ones while taking its overhead into account. We showed that significant gains can be achieved under the assistance of a narrow-band channel, which periodically broadcasts channel-status information to facilitate CRs calculating their multi-level spectrum opportunity. Currently our work only applies to single-hop ad hoc CRNs. Our future efforts will include the routing into the problem for a multi-hop environment.

Acknowledgements

This research was supported in part by NSF (under grants CNS-0904681, CNS-0721935, and IIP-0832238), Raytheon, and Connection One (an I/UCRC NSF/industry/university consortium). Any opinions, findings, conclusions, or recommendations expressed in this paper are those of the author(s) and do not necessarily reflect the views of the National Science Foundation. Part of this work was conducted while M. Krunz was a visiting researcher at the Universidad Carlos III de Madrid and IMDEA Networks.

References

[1] L. Cao and H. Zheng. Distributed spectrum allocation via local bargaining. In *Proceedings of IEEE Communications Society Conference on Sensor, Mesh and Ad Hoc Communications and Networks (SECON)*, 2005.

[2] L. Cao and H. Zheng. On the efficiency and complexity of distributed spectrum allocation. In *Proceedings of International Conference on Cognitive Radio Oriented Wireless Networks and Communications*, 2007.

[3] N. B. Chang and M. Liu. Optimal channel probing and transmission scheduling for opportunistic spectrum access. In *Proceedings of the ACM MobiCom Conference*, 2007.

[4] FCC Document 08-260. Second report and order and memorandum opinion and order: In the matter of unlicensed operation in the TV broadcast bands and additional spectrum for unlicensed devices below 900 MHz and in the 3 GHz band, Nov. 2008.

[5] Y. T. Hou, Y. Shi, and H. D. Sherali. Optimal spectrum sharing for multi-hop software defined radio networks. In *Proceedings of the IEEE INFOCOM Conference*, pages 1–9, 2007.

[6] S. Huang, X. Liu, and Z. Ding. Opportunistic spectrum access in cognitive radio networks. In *Proceedings of the IEEE INFOCOM Conference*, pages 1427–1435, Apr. 2008.

[7] J. Jia, Q. Zhang, and X. Shen. HC-MAC: A hardware-constrained cognitive MAC for efficient spectrum management. *IEEE Journal on Selected Areas in Communications*, 26(1):106–117, Jan. 2008.

[8] H. Kim and K. G. Shin. Efficient discovery of spectrum opportunities with mac-layer sensing in cognitive radio networks. *IEEE Transactions on Mobile Computing*, 7(5):533–545, May 2008.

[9] J. Lee, R. V. Sonalkar, and J. M. Cioffi. Multiuser bit loading for multicarrier systems. *IEEE Transactions on Communications*, 54(7):1170–1174, July 2006.

[10] Y. Shi and Y. T. Hou. Optimal power control for multi-hop software defined radio networks. In *Proceedings of the IEEE INFOCOM Conference*, pages 1694–1702, 2007.

[11] Y. Shi and Y. T. Hou. A distributed optimization algorithm for multi-hop cognitive radio networks. In *Proceedings of the IEEE INFOCOM Conference*, pages 1966–1974, Apr. 2008.

[12] T. Shu and M. Krunz. Joint power/rate controrl and channel assignment in cognitive radio networks: a multi-leveled spectrum opportunity perspective. *Technical Report of the University of Arizona, available at http://www.ece.arizona.edu/∼krunz*, Aug. 2008.

[13] T. Starr, M. Sorbara, J. M. Cioffi, and P. J. Silverman. *DSL Advances*. Prentice-Hall, 2003.

[14] M. Venkatachalam, K. Etemad, W. Ballantyne, and B. Chen. Location services in WiMAX networks. *IEEE Communications Magazine*, pages 92–98, Oct. 2009.

[15] W. Wang and X. Liu. List-coloring based channel allocation for open-spectrum wireless networks. In *Proceedings of the IEEE Vehicular Tech. Conference*, pages 690–694, 2005 Fall.

[16] Y. Xing, R. Chandramouli, S. Mangold, and S. N. Shankar. Dynamic spectrum access in open spectrum wireless networks. *IEEE Journal on Selected Areas in Communications*, 24(3):626–637, Mar. 2006.

[17] Y. Xing, C. N. Mathur, M. A. Haleem, R. Chandramouli, and K. P. Subbalakshmi. Dynamic spectrum access with QoS and interference temperature constraints. *IEEE Transactions on Mobile Computing*, 6(4):423–433, Apr. 2007.

[18] Y. Yuan, P. Bahl, R. Chandra, T. Moscibroda, and Y. Wu. Allocating dynamic time-spectrum blocks in cognitive radio networks. In *Proceedings of the ACM MobiHoc Conference*, pages 130–139, 2007.

[19] J. Zhao, H. Zheng, and G. Yang. Distributed coordination in dynamic spectrum allocation networks. In *Proceedings of the IEEE Symposium on New Frontiers in Dynamic Spectrum Access Networks (DySPAN)*, 2005.

[20] Q. Zhao, S. Geirhofer, L. Tong, and B. M. Sadler. Optimal dynamic spectrum access via periodic channel sensing. In *Proceedings of the IEEE WCNC Conference*, 2007.

[21] Q. Zhao, L. Tong, A. Swami, and Y. Chen. Decentralized cognitive mac for opportunistic spectrum access in ad hoc networks: A POMDP framework. *IEEE Journal on Selected Areas in Communications*, 25(3):589–600, Apr. 2007.

[22] H. Zheng and L. Cao. Device-centric spectrum management. In *Proceedings of the IEEE Symposium on New Frontiers in Dynamic Spectrum Access Networks (DySPAN)*, 2005.

[23] H. Zheng and C. Peng. Collaboration and fairness in opportunistic spectrum access. In *Proceedings of the IEEE ICC Conference*, 2005.